$$xHFe_4(CH)(CO)_{12}(ads) \xrightarrow[-CO]{slow} yHFe_4(CH)(CO)_{12}(ads) + (x-y)HFe_4(CH)(CO)_{11}(ads) \xrightarrow[-CO]{fast} yHFe_4(CH)(CO)_{12}(ads) + Fe(ads)\ (or\ FeC(ads)) \quad (7)$$

for the activation of metal carbonyls by attached ligands are known.[41]

To further explore the nature of the surface carbonyl species, the reactions of CO/H_2 and of benzene/H_2 over the supported cluster were investigated. In a batch reactor, the CO/H_2 mixture did not produce reduction products of CO below 175 °C, and at that temperature the product distribution appeared to be similar to that produced in conventional Fischer–Tropsch chemistry. Apparently at these high temperatures, the surface species closely approximates bulk iron or iron carbide. The surface species have activity for benzene hydrogenation at lower temperatures, but cyclohexane was the only significant product, and therefore no evidence exists from this experiment for catalytic ensembles that differ from the bulk metal in catalytic properties.

Acknowledgment. We appreciate the support of DOE (Grant DE-AC02-83ER13104) for studies on the characterization of surface species and the Gas Research Institute (Grant 5082-260-0693) for studies on the reactivity of the adsorbed clusters. P.M.B. thanks Paula Bogdan and Andrew Lang for assistance in collecting EXAFS data. D.F.S. thanks the John Simon Guggenheim Foundation for a fellowship.

Registry No. $HFe_4(CH)(CO)_{12}$, 74792-06-6; $[HFe_4(C)(CO)_{12}]^-$, 74792-02-2; Al_2O_3, 1344-28-1; CO, 630-08-0.

---

[41] Butts, S. B.; Strauss, S. H.; Holt, E. M.; Stimson, R. E.; Alcock, N. W.; Shriver, D. F. *J. Am. Chem. Soc.* **1980**, *102*, 5093. Richmond, T. G.; Basolo, F.; Shriver, D. F. *Inorg. Chem.* **1982**, *21*, 1272.

Contribution from the Departments of Chemistry, Wayne State University,
Detroit, Michigan 48202, and Martin-Luther University, 402 Halle(s), G.D.R.

Synthetic and Spectroscopic Studies into the Mechanism of the $[Pt(PR_3)_4]/R_2P(S)H$ Reaction. Formation and Structure of the Novel Diplatinum(II) Dihydride Complex $[Pt_2(H)_2(P\text{-}t\text{-}Bu_3)_2(\mu\text{-}SPPh_2)_2]$

A. F. M. M. RAHMAN,[1a] C. CECCARELLI,[1a] J. P. OLIVER,*[1a] B. MESSBAUER,[1b] H. MEYER,[1b] and B. WALTHER*[1b,2]

Received May 25, 1984

The reaction of $[Pt(PR'_3)_4]$ (R′ = alkyl, phenyl) with $Ph_2P(S)H$ yields the diplatinum(I) complexes $[Pt_2(PR'_3)_2(\mu\text{-}SPPh_2)_2]$. The reaction proceeds via the isolable intermediate $[PtH(PR'_3)_2\{P(S)Ph_2\}]$ which exists in solution as a mixture of the trans and cis isomers. Both isomers lose one phosphine ligand at higher temperatures, yielding coordinately and electronically unsaturated species that form the final diplatinum(I) complexes. The intermediates have been characterized by NMR spectroscopy and the results discussed in comparison to the reaction of $[Pt(PR'_3)_4]$ with $Ph_2P(O)H$. $[Pt(P\text{-}t\text{-}Bu_3)_2]$ and $Ph_2P(S)H$ react unexpectedly to give the novel diplatinum(II) complex $[Pt_2(H)_2(P\text{-}t\text{-}Bu_3)_2(\mu\text{-}SPPh_2)_2]$ which has been characterized by ^{31}P and ^1H NMR spectroscopy and by a single-crystal structure determination. It crystallizes in the monoclinic system, space group $C2/c$, with cell dimensions of a = 18.063 (1) Å, b = 16.572 (1) Å, c = 17.318 (1) Å, β = 92.240 (5)°, V = 5180.1 (6) $Å^3$, and Z = 4. Full-matrix least-squares refinement on 2362 data gave R = 3.5% and R_w = 4.6%. The structure determination has shown that the platinum(II) atoms have square-planar geometry surrounded by bridging S and P atoms and terminal P and H atoms and that the Pt–S–P(1)′–Pt′–S′–P(1) unit is in a boat conformation. Each of the Pt–S–P(1)′–Pt′ units is planar. The planar atoms in the dimer are 3.620 (1) Å apart, ruling out the possibility of metal–metal interactions. The other distances around Pt are as follows: Pt–S = 2.451 (3) Å, Pt–P(1)(bridge) = 2.285 (3) Å, Pt–P(2)(terminal) = 2.330 (3) Å, and Pt–H(66) = 1.42 Å.

Introduction

Secondary phosphine chalcogenides, $R_2P(E)H$ (E = O, S, Se), form different types of derivatives when reacted with (tertiary phosphine)platinum(0) complexes, $[Pt(PR'_3)_4]$. Thus, if E = O mononuclear complexes containing the uninegative bidentate hydrogen-bridged ligand $(Ph_2PO\cdots H\cdots OPPh_2)^-$ are formed according to eq 1.[3] If, however, E = S or Se, bis(chalcogenophosphinito)-bridged diplatinum(I) complexes result as outlined in eq 2.[4]

$$[Pt(PR'_3)_4] + 2R_2P(O)H \rightarrow [PtH(PR'_3)\{(R_2PO)_2H\}] + 3PR'_3 \quad (1)$$

$$2[Pt(PR'_3)_4] + 2R_2P(E)H \xrightarrow{E\,=\,S,\,Se} [Pt_2(PR'_3)_2(\mu\text{-}EPR_2)_2] + 6PR'_3 + H_2 \quad (2)$$

The first reaction involves an oxidative-addition step to form $[Pt^{II}H(PR'_3)_2\{P(O)R_2\}]$ which (either in a conserted or subsequent step) substitutes $R_2P(O)H$ for one PR'_3 ligand. The driving force for this latter step is the formation of the strong hydrogen bond. Reaction 2 is unique in that treatment of $[Pt(PR'_3)_4]$ with a protic acid yields a diplatinum(I) complex. Therefore, we have undertaken a study to elucidate the mechanism of this reaction. This paper reports attempts to characterize the key intermediate of reaction 2, $[PtH(PR'_3)_2\{P(S)R_2\}]$. In the course of this study we unexpectedly found that treatment of $[Pt(P\text{-}t\text{-}Bu_3)_2]$ with $Ph_2P(S)H$ yields the novel diplatinum(II) dihydride complex, $[Pt_2(H)_2(P\text{-}t\text{-}Bu_3)_2(\mu\text{-}SPPh_2)_2]$, whose structure has been established by single-crystal X-ray analysis.

Experimental Section

General Procedures. All reactions were carried out anaerobically by using conventional Schlenk techniques. Solvents were dried, deoxygenated, and distilled just prior to use. Starting materials were prepared according to literature procedures: $[Pt(PMePh_2)_4]$,[5] $[Pt(P\text{-}t\text{-}Bu_3)_2]$,[6] $Ph_2P(S)H$.[7] Details of the NMR measurements are given elsewhere.[8]

***trans/cis*-$[Pt(H)(PMePh_2)_2\{P(S)Ph_2\}]$ (1a/1b).** A 218-mg (1 mmol) sample of solid $Ph_2P(S)H$ was added to a solution of 995 mg (1 mmol) of $[Pt(PMePh_2)_4]$ in 40 mL of toluene at −20 °C. After 4 h of stirring at −20 °C, the solution was filtered into 70 mL of *n*-pentane that had been cooled to −60 °C. The precipitate was filtered off at −70 °C, washed with 40 mL of diethyl ether precooled to −60 °C, and dried 8 h

---

[1] (a) Wayne State University. (b) Martin-Luther University.

[2] Secondary Phosphine Chalcogenides. 9. Part 8: Zschunke, A.; Meyer, H.; Heidlas, I.; Messbauer, B.; Walther, B.; Schadler, H.-D.; Thomas, B. *Z. Anorg. Allg. Chem.* **1983**, *504*, 117.

[3] Beaulieu, W. B.; Rauchfuss, T. B.; Roundhill, D. M. *Inorg. Chem.* **1975**, *14*, 1732.

[4] Walther, B.; Messbauer, B.; Meyer, H. *Inorg. Chim. Acta* **1979**, *37*, L525.

[5] Mukhedkar, A. J.; Green, M.; Stone, F. G. A. *J. Chem. Soc. A* **1969**, 3023.

[6] Goel, R. G.; Ogini, W. P.; Srivastava, R. C., *J. Organomet. Chem.* **1981**, *214*, 405.

[7] Peters, G., *J. Org. Chem.* **1962**, *27*, 2198.

[8] Messbauer, B.; Meyer, H.; Walther, B.; Heeg, M. J.; Rahman, A. F. M. M.; Oliver, J. P. *Inorg. Chem.* **1983**, *22*, 272.

Table I. Experimental Data from the X-ray Diffraction Study on $[Pt\{\mu\text{-}SP(C_6H_5)_2\}P\{C(CH_3)_3\}_3H]_2$

mol formula: $Pt_2S_2P_4C_{43}H_{76}$
mol wt: 615.669
cryst system: monoclinic
space gp: $C2/c$
cell dimens
a = 18.063 (1) Å
b = 16.572 (1) Å
c = 17.318 (1) Å
β = 92.240 (5)°
V = 5180.1 (6) Å^3
Z = 4
D(calcd) = 1.579 g cm^{-3}
radiation: Mo K$\bar{\alpha}$ (λ = 0.71069 Å)
monochromator: graphite
rflcns measd: $+h,+k,\pm l$
2θ range: 4–45°
scan type: θ–2θ, moving crystal–moving counter
scan width: $[2\theta(\text{Mo K}\alpha_1) - 1.0]$–$[2\theta(\text{Mo K}\alpha_2) + 1.0]$
no. of std reflcns: $3(\bar{1}\bar{1}3; 0\bar{4}0; 310)$ measd every 97 reflcns; no signif dev from the mean obsd
no. of unique data: 7021
no. of unique data with $F^2 > 3.0\sigma(I)$: 2876
abs coeff: 56.804 cm^{-1}
$F(000) = 2448e$
R = 0.035
R_w = 0.046
NV = 253

on a high-vacuum line (10^{-5} mm) at −60 °C; yield 600 mg (74%).

$[Pt_2(H)_2(P\text{-}t\text{-}Bu_3)_2(\mu\text{-}SPPh_2)_2]$ (2). Solid $Ph_2P(S)H$ (167 mg, 0.76 mmol) was added to a solution of 457 mg (0.76 mmol) of $[Pt(P\text{-}t\text{-}Bu_3)_4]$ in 20 mL of benzene. The golden yellow solution rapidly turned pale yellow. After stirring for 12 h, the volume of the solution was reduced to 5 mL. Colorless crystals (0.49 g, 85%) were filtered off, washed with cold *n*-pentane, and recrystallized from benzene; mp 233–234 °C dec. Further product (ca. 0.5 g) was obtained from the filtrate after standing in a refrigerator. **2** is soluble in CH_2Cl, $CHCl_3$, acetone, tetrahydrofuran, C_6H_6, and diethyl ether but sparingly soluble in *n*-pentane. **2** analyzed satisfactorily.

X-ray Data Collection. An orange-yellow crystal of approximate size 0.27 × 0.24 × 0.30 mm^3 was mounted on a Syntex P2$_1$ automatic X-ray diffractometer and a data set collected. All experimental parameters and conditions are listed in Table I. The final cell constants were obtained by least-squares refinement of 78 strong reflections with 2θ between 15 and 25°.

Solution and Refinement of the Structure. Initial efforts were made to solve the structure in space group $P2_1/c$ from 2876 reflections with $I > 3\sigma(I)$ collected in the region $4° < 2\theta < 45°$ with $h,k,\pm l$, but no satisfactory solution could be found. It was then noted that $h + k$ odd reflections were either very weak or absent, indicating the space group $C2/c$. Subsequently all reflections with $h + k$ odd were deleted, and the structure was solved by heavy-atom methods.

Solution of the three-dimensional Patterson function gave the position of the platinum atom in the asymmetric unit. Subsequently Fourier and difference syntheses established the positions of the remaining non-hydrogen atoms.[9] Gaussian integration absorption corrections were applied (μ = 56.804 cm^{-1}); the correction factor ranged from 3.185 to 4.314. Positions and temperature factors of all non-hydrogen atoms were refined by the least-squares technique. Hydrogen atoms were placed in calculated positions and were adjusted after every second least-squares cycle and given arbitrary isotropic temperature factors of 4.0 Å. All parameters associated with hydrogen were held fixed throughout the refinement. Full-matrix least-squares refinement using our usual weighing scheme[10] yielded residual indices of R = 0.035 and R_w = 0.046. The position of the hydrogen bonded to platinum was located from the final difference map, but no attempt was made to refine its position. The only other large peak on the final difference map was located 1.045 Å away from the Pt atom with an electron density of 0.99 e/Å^3. Other parameters from the final least-squares cycle are given in Table I.

Table II. Atomic Coordinates for the Non-Hydrogen Atoms in the $[Pt(\mu\text{-}SPPh_2)(H)(P\text{-}t\text{-}Bu_3)]_2$ Molecule

atom	x	y	z
Pt	−0.07748 (2)	0.20129 (2)	0.18049 (2)
S	−0.1066 (2)	0.2947 (2)	0.2848 (2)
P(1)	0.0149 (2)	0.2852 (1)	0.1432 (2)
P(2)	−0.1747 (2)	0.1092 (2)	0.1845 (2)
C(1)	−0.0190 (6)	0.3860 (6)	0.1243 (6)
C(2)	−0.0859 (10)	0.3991 (9)	0.0885 (11)
C(3)	−0.1140 (12)	0.4767 (11)	0.0737 (11)
C(4)	−0.0725 (11)	0.5404 (9)	0.0928 (11)
C(5)	−0.0120 (11)	0.5294 (10)	0.1305 (19)
C(6)	0.0151 (9)	0.4525 (9)	0.1505 (16)
C(7)	0.0482 (7)	0.2612 (6)	0.0472 (6)
C(8)	0.1224 (8)	0.2683 (8)	0.0297 (7)
C(9)	0.1443 (9)	0.2528 (10)	−0.0460 (11)
C(10)	0.0951 (14)	0.2311 (9)	−0.1014 (10)
C(11)	0.0217 (10)	0.2248 (9)	−0.0863 (8)
C(12)	−0.0021 (8)	0.2384 (9)	−0.0128 (7)
C(13)	−0.1716 (9)	0.0359 (8)	0.0999 (8)
C(14)	−0.2298 (9)	−0.0291 (9)	0.0932 (9)
C(15)	−0.1730 (11)	0.0810 (12)	0.0248 (9)
C(16)	−0.1005 (13)	−0.0072 (13)	0.0981 (18)
C(17)	−0.2680 (8)	0.1657 (10)	0.1738 (9)
C(18)	−0.3357 (9)	0.1163 (11)	0.1697 (13)
C(19)	−0.2768 (10)	0.2295 (17)	0.2251 (18)
C(20)	−0.2709 (16)	0.2097 (21)	0.1013 (18)
C(21)	−0.1742 (10)	0.0469 (11)	0.2772 (9)
C(22)	−0.2298 (10)	−0.0179 (10)	0.2865 (8)
C(23)	−0.1744 (29)	0.0955 (18)	0.3407 (12)
C(24)	−0.1018 (16)	0.0135 (29)	0.2894 (24)
H(66)[a]	−0.0590	0.1580	0.0267

[a] H(66) coordinates were taken from the final difference map and are unrefined.

Table III. Selected Interatomic Distances and Angles in the $[Pt(\mu\text{-}SPPh_2)(H)(P\text{-}t\text{-}Bu_3)]_2$ Molecules

atoms	dist, Å	atoms	dist, Å
Pt–S	2.451 (3)	P(1)–C(1)	1.804 (10)
Pt–P(1)	2.285 (3)	P(1)–C(7)	1.834 (11)
Pt–P(2)	2.330 (3)	P(2)–C(13)	1.906 (12)
Pt–H(66)[a]	1.42	P(2)–C(17)	1.931 (16)
S–P(1)	2.040 (4)	P(2)–C(21)	1.910 (13)
atoms	**angles, deg**	**atoms**	**angles, deg**
S–Pt–P(1)	90.2 (1)	Pt–P(2)–C(13)	110.5 (5)
S–Pt–P(2)	102.0 (1)	Pt–P(2)–C(17)	109.6 (5)
P(1)–Pt–P(2)	165.2 (1)	Pt–P(2)–C(21)	113.6 (5)
Pt–S–P(1′)	102.1 (1)	C(13)–P(2)–C(17)	106.7 (7)
Pt–P(1)–S′	117.3 (1)	C(13)–P(2)–C(21)	107.6 (8)
Pt–P(1)–C(1)	111.6 (3)	C(17)–P(2)–C(21)	108.6 (8)
S′–P(1)–C(1)	107.6 (4)	H(66)–Pt–P(1)[a]	83.0
S′–P(1)–C(7)	106.5 (4)	H(66)–Pt–P(2)[a]	84.0
C(1)–P(1)–C(7)	99.0 (5)	H(66)–Pt–S[a]	171.1

[a] The distance and angles involving the H atom bound to Pt are unrefined.

Neutral-atom scattering factors were used, and that for Pt was corrected for anomalous dispersion.[11] Final positional parameters are presented in Table II. Selected interatomic distances and angles are listed in Table III. The errors were estimated by the variance–covariance method. Lattice errors were not included. Full listings of interatomic distances and angles (Table S-I), anisotropic thermal parameters (Table S-II), hydrogen atom positional parameters (Table S-III), least-squares planes (Table S-IV), and observed and calculated structure amplitudes (Table S-V) are available.[12]

Results

Syntheses. Protic acids, HX, can react with $[M(PR_3)_4]$ (M = Pd, Pt) by a variety of different pathways typified by those outlined in eq 3 with formation of a complex containing the metal atom in either the 2+ or 4+ oxidation state depending on M, the acid strength of HX, the ligating properties of X, the solvent, and

---

(9) Computing programs were local modifications of Templeton's ABSORB, Zalkin's FORDAP, Johnson's ORTEP, Busing-Martin-Levy's ORFLS and ORFEE, and Zalkins's HFINDR.

(10) The weighting scheme is given by $w = 1/\sigma^2(F_o)^2$, with the function minimized $\sum w(|F_o| - |F_c|)^2$.

(11) "International Tables fr X-ray Crystallography", 3rd ed.; Kynoch Press: Birmingham, England, 1969; Vol. 1.

(12) See paragraph at the end of the paper regarding supplementary material.

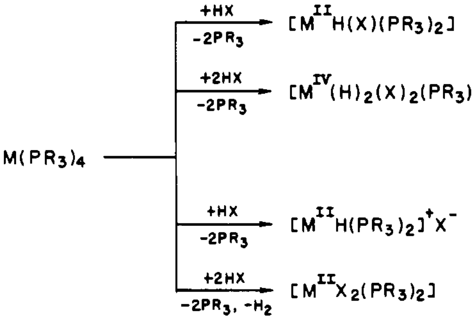

(3)

the reaction conditions. Secondary phosphine sulfides and selenides do not react in any of these ways but form bis(chalcogenophosphinito)-bridged dimetal(I) complexes directly when treated with $[M(PR_3)_4]$ in benzene at room temperature, eq 2.[4] Carrying out the reaction of $Ph_2P(S)H$ with $[Pt(PMePh_2)_4]$ at −20 °C in toluene allows isolation of colorless $[PtH(PMePh_2)_2\{P(S)Ph_2\}]$ (**1**) which in solution appears to be a mixture of the trans (**1a**) and the cis (**1b**) isomers. **1a** is the product of the oxidative-addition reaction of $Ph_2P(S)H$ and $[Pt(PMePh_2)_2]$. The latter results from the dissociation of $[Pt(PMePh_2)_4$. **1b** likely follows from a **1a** → **1b** rearrangement. The analogous palladium complexes could neither be isolated nor spectroscopically detected in solution, probably due to the lower stability of the palladium hydride complexes. Above ca. −10 °C solid **1** and its solutions slowly release dihydrogen to give the final complex $[Pt_2(PMePh_2)_2(\mu\text{-}SPPh_2)_2]$.

In order to obtain a $[PtH(PR'_3)_2\{P(S)R_2\}]$ complex of higher thermal stability, the complex $[Pt(P\text{-}t\text{-}Bu_3)_2]$, with bulky $P\text{-}t\text{-}Bu_3$ auxiliary ligands, was reacted with $Ph_2P(S)H$. Rather surprisingly, the novel diplatinum(II) dihydride complex $[Pt_2(H)_2(P\text{-}t\text{-}Bu_3)_2(\mu\text{-}SPPh_2)_2]$ (**2**) was formed in high yield in the course of both an oxidative-addition and dimerization reaction (eq 4).

$$2Ph_2P(S)H + 2[Pt(P\text{-}t\text{-}Bu_3)_2] \xrightarrow{-2P\text{-}t\text{-}Bu_3} [Pt_2(H)_2(P\text{-}t\text{-}Bu_3)_2(\mu\text{-}SPPh_2)_2] \quad (4)$$

Description of the Structure. The crystal structure of $[Pt(\mu\text{-}SPPh_2)(P\text{-}t\text{-}Bu_3)H]_2$, shown in Figure 1, consists of discrete dimeric molecules, separated by normal van der Waals distances. The closest nonbonding intermolecular distance observed is 2.105 Å between H(51) and H(183)′ of a different molecule. The closest nonbonding distance, ignoring hydrogens, is 3.536 (23) Å between C(5) and C(18)′ of a different molecule. Hence, the molecular structure appears to be relatively unaffected by packing interactions.

The molecule can be formally regarded as a complex of Pt(II) consisting of two nearly planar $\{Pt(\mu\text{-}SPPh_2)(P\text{-}t\text{-}Bu_3)H\}$ units (Table S-IV) in which none of the atoms directly bonded to the platinum deviate from the plane containing them and the metal by more than ±0.054 Å. These two units are linked by bridging $SPPh_2^-$ anions. Further, in the central six-atom framework the two Pt–S–P′–Pt′ and Pt–P–S′–Pt′ units are essentially planar (Table S-IV) with a dihedral angle between them of 97.5°. This is clearly illustrated in Figure 1. The Pt–Pt distance of 3.620 (1) Å in this compound indicates there is no metal–metal interaction. The Pt–S distance of 2.451 (3) Å is significantly longer than the Pt–S bonds in similar compounds. The Pt–P(1)(bridging) and Pt–P(2)(terminal) distances are 2.285 (3) and 2.330 (3) Å, respectively, and are within the normal range observed for similar bonds. The S–P(1)′ bonding distance of 2.040 (4) Å is only slightly shorter than that of 2.090 (5) Å found in P_4S_3.[13] The fourth position on the Pt atom completing the square-planar geometry is occupied by the H atom. The distance obtained from the difference map of 1.42 Å is short, but no effort was made to refine this position because of the inherent difficulties of obtaining good metal–hydrogen distances by X-ray diffraction studies in systems of this type.

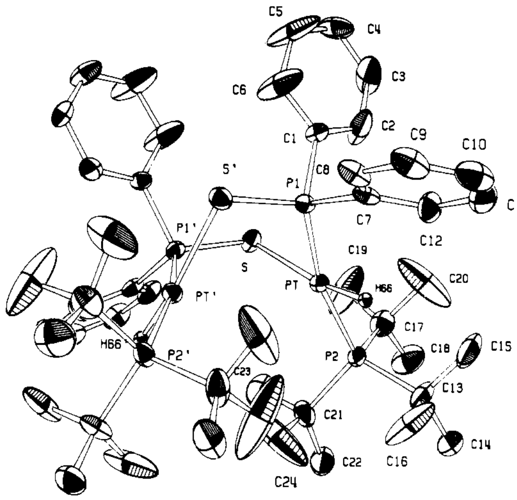

Figure 1. ORTEP diagram of $[Pt(\mu\text{-}SPPh_2)(H)(P\text{-}t\text{-}Bu_3)]_2$ with the atoms labeled. The diagram has 25% thermal ellipsoids. The hydrogen atoms, with the exception of that bound to Pt, have been omitted for sake of clarity.

The distorted tetrahedral geometry about the bridging phosphorus atoms is shown from the data in Table III. Thus, the Pt–P(1)–C(1) and Pt–P(1)–C(7) angles of 111.6 (3) and 113.2 (4)°, respectively, result in a correspondingly smaller value of 99.0 (5)° for the C(1)–P(1)–C(7) angle, with the phenyl groups tilted away from the center of the molecule and slightly inclined to each other. The dihedral angle between the planes containing the rings is 82.4°. This serves to minimize steric crowding near the central six-membered Pt–S–P(1)′–Pt′–S′–P(1) framework. The bridge angle Pt–P(1)–S′ of 117.3 (1)° deviates from the tetrahedral value probably to minimize the strain in the six-atom central framework. The average P(1)–C(phenyl) distance of 1.82 (1) Å appears to be normal.

Only a few structures of complexes containing a central $M_2(\mu\text{-}EPR_2)_2$ unit have been reported, and they have been shown to adopt quite different ring conformations: $[Re_2(CO)_8(\mu\text{-}OPMe_2)_2]$, distorted chair;[14] $[Mn_2(CO)_8(\mu\text{-}OPPh_2)_2]$, twisted boat;[15] $[Ni_2(\eta^5\text{-}Cp)_2(\mu\text{-}SPMe_2)_2]$, ideal chair;[16] $[Pt_2(S_2CN\text{-}i\text{-}Pr_2)_2(\mu\text{-}SPPh_2)_2]\cdot 2CHCl_3$, chair.[17] **2** obviously adopts the boat conformation in order to minimize repulsion between the phenyl groups on the bridging phosphorus atoms and the bulky *tert*-butylphosphine ligands on the platinum atoms. This repulsion makes the C(1)–P(1)–C(7) angle fairly small compared with the 103.11° found for $[Pt_2(SCN\text{-}i\text{-}Pr_2)_2(\mu\text{-}SPPh_2)_2]\cdot 2CHCl_3$.[17] The rather long Pt–P and Pt–S bonds in compound **2** compared to those in $[Pt_2(S_2CN\text{-}i\text{-}Pr_2)_2]\cdot 2CHCl_3$, 2.225 and 2.313 Å, respectively,[17] indicate that weaker bonds exist between the monomeric units in **2**. This dihedral angle between the plane defined by the four bridging atoms is similar for **2**, $[Ni_2(\eta^5\text{-}Cp)_2(\mu\text{-}SPMe_2)_2]$ (56.1°)[16] and $[Pt_2(S_2CN\text{-}i\text{-}Pr_2)_2(\mu\text{-}SPPh_2)_2]\cdot 2CHCl_3$ (54°).[17] The P–S bond length corresponds also to those observed for dipalladium(I) and diplatinum(I) complexes of type $(M_2L_2(\mu\text{-}SPPh_2)_2]$[8,18] and indicates some π-bond character.

Spectra. Although no attempts have been made to subject **1** to elemental analysis, its composition and structure clearly follow from the IR and ^{31}P and ^{1}H NMR spectral data summarized in Table IV. The $^{31}P\{^1H\}$ and ^{1}H NMR spectra display the individual signals of **1a** and **1b** only at low temperatures (intensity ratio ca. 7:3). The assignments of the signals of the ^{31}P NMR

---

(13) Leung, Y. H.; Waser, J.; van Houten, S.; Vos, A.; Wiegers, G. A.; Wiebenga, E. H. *Acta Crystallogr.* **1957**, *10*, 5741.

(14) Mundig, G.; Schilling, B.; Weishaupt, M.; Lindner, E.; Straähle, J. *Z. Anorg. Allg. Chem.* **1977**, *437*, 169.

(15) Hoehne, S.; Lindner, E.; Schilling, B., *J. Organomet. Chem.* **1977**, *139*, 315.

(16) Lindner, E.; Bonachir, F.; Hiller, W. *J. Organomet. Chem.* **1981**, *210*, C37.

(17) Anderson, D. M.; Ebsworth, E. A. V.; Stephenson, T. A.; Walkinshaw, M. D. *J. Chem. Soc., Dalton Trans.* **1982**, 2343.

(18) Wagner, K. P.; Hess, R. W.; Treichel, P. M.; Calabrese, J. C. *Inorg. Chem.* **1975**, *14*, 1121.

Table IV. Spectroscopic Data for Compounds **1a**, **1b**, and **2**[a]

		^{31}P NMR					^{1}H NMR					
no.		δ(P^1)	δ(P^2)	δ(P^3)	^1J(PtP)	^2J(PP)	δ(PtH)	δ(CH_3)	^1J(PtH)	^1J(*trans*-PH)	^2J(*cis*-PH)	IR ν(PtH)
1a	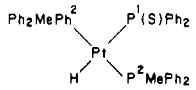	43.b[b,c]	8.62[d]	...	2147 (P^1) 2863 (P^2)	21.2	−5.97[b,h]	0.97[j]	773.8	166.5	30.1	2150[l]
1b	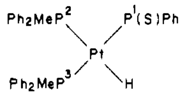	38.94[e]	20.42	3.52[f]	ca. 3163 (P^1) ca. 2530 (P^3) ca. 2079 (P^2)	371 (P^1P^3) 20.5 (P^1P^2)[g]	−4.36[i]	*k*	932	178.4	ca. 20	
2	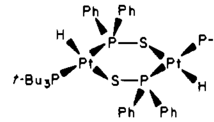	44.46[m] ($P^{1,2}$)	...	83.79 ($P^{3,4}$)	2745.2 ($P^{3,4}$)[n] 2930.7 ($P^{1,2}$)[o]	417.2 (P^1P^4, P^2P^3)[p]	−12.7[q]	1.32[h]	1095	...	20.2 4.7	2285[r]

[a] δ in ppm, *J* in Hz, ν in cm^{-1}. [b] Toluene-d_8: 1931 (^{31}P), 1831 (^{1}H). [c] Unresolved triplet. [d] Doublet by ^{2}*Jncis*-PP). [e] Doublets of doublets by $^2J(P^1P^3)$ and $^2J(P^1P^2)$. [f] Doublet by $^2J(P^1P^3)$. [g] Observed in the P^1 signal only. [h] Doublet of triplets flanked by the Pt satellites. [i] Doublet by ^1J(*trans*-PH), ^2J(*cis*-PH) not resolved. [j] Virtual 1:2:1 triplet; $N = J(AX) + J(A'X) \sim {}^2J(PCH) = 12.7$ Hz; ^{J}(PtPCH) not observed. [k] Not observed due to low intensity and obscurity by the signal of diethyl ether used in the sample preparation. [l] CH_2Cl_2. [m] C_6D_6/C_6H_6. [n] $^4J(PtP^{3,4}) = 31.7$ Hz. [o] $^2J(PtP^{1,2}) = 25.0$ Hz. [p] $^3J(P^1P^2) = 45.3$ Hz. [q] C_6D_6. [r] KBr, ν(PS) 570 cm^{-1}.

spectrum were confirmed by double-resonance experiments. Increasing temperature causes the following changes in the NMR spectra: (i) In the $^{31}P\{^1H\}$ spectrum, the ^2J(PP) couplings of both **1a** and **1b** disappear but the individual signals of both isomers are still observable at 253 K. A small excess of $PMePh_2$ (which might stem from the synthesis if not carefully removed) caused the ^2J(PP) couplings to disappear as a result of fast chemical exchange. A large excess of $PMePh_2$ results in a spectrum showing only a broad signal between −5 and −15 ppm for the coordinated and noncoordinated $PMePh_2$ ligands. (ii) In the ^{1}H NMR spectrum, the intensity of the hydride signal of **1a** decreases slowly with time and increasing temperature but is still observable at 323 K, showing the slowness of the hydrogen-release process. (iii) The ^2J(*cis*-PH) coupling of **1a** disappears at ca. 200 K, whereas the chemical shift, as well as ^1J(PtH) and ^2J(*trans*-PH) remain essentially unchanged over the range of temperature studied. The doublet splitting of **1b** by ^2J(*trans*-PH) collapses at ca. 273 K into a broade signal at ca. −4.9 ppm. (iv) The CH_3 resonance of **1a** shifts to higher field (0.86 ppm at 283 K) and decreases in intensity. At 253 K (and after the time necessary to record the spectra) a second CH_3 resonance appears at 0.99 ppm that is assigned to the methyl resonance of the final diplatinum complex, $[Pt_2(PMePh_2)_2(\mu\text{-}SPPh_2)_2]$ (eq 2).

The solid-state structure of **2** appears to be maintained in solution as established by its $^{31}P\{^1H\}$ and ^{1}H NMR spectra (Table IV). Of the three isotopomers only the AA′MM′ subspectrum (43.8%, AA′ and MM′ terminal and bridging phosphorus nuclei, respectively) and the AA′MM′X subspectrum (44.8%, AA′ terminal, MM′ bridging phosphorus nuclei, X ^{195}Pt nucleus) could be analyzed in the ^{31}P NMR spectrum. The subspectrum of the third isotopomer AA′MM′XX′ (11.4%) is obscured by the AA′MM′X subspectrum, preventing the determination of the $^{195}Pt^{195}Pt$ coupling constant; however, it follows from the spectral simulation that this coupling should be in the range of 0–100 Hz. The long-range PtP couplings, as well as $^3J(P^1P^2)$, confirm the dinuclear structure. The zero coupling observed between the terminal phosphorus nuclei, $^5J(P^3P^4)$, should be compared to the coupling of the terminal phosphorus nuclei in diplatinum(I) complexes of type $[Pt_2(PR'_3)_2(\mu\text{-}SPR_2)_2]$, which are found to be in the range of 188 Hz up to 650 Hz.[19] This strongly supports the concept that the coupling observed in the diplatinum(I) complexes is in fact a three-bond coupling constant, ^3J(PP), transmitted through the PtPt bond. The NMR data for **2** may be compared with those of $[Pt_2(S_2CNEt_2)_2(\mu\text{-}(SPPh_2)_2]$ (δ 30.5, $^1J(PtP) = 3656.4$, $^2J(PtP) = 13.6$, $^3J(PtPt) = 940$ Hz).[14] The differences, the most obvious being that one of the ^3J(PtPt) values, may be due to both the different trans ligands and the change of the ring conformation. The ^{1}H NMR spectrum confirms the trans position of the hydrido ligands relative to the sulfur atoms from the small ^2J(PH) coupling observed. No loss of intensity of the hydride signal could be observed after 1 h at 373 K.

Discussion

The mechanism of the $[Pt(PR'_3)_4]/R_2P(S)H$ reaction involves a fast oxidative addition of $R_2P(S)H$ on the coordinatively unsaturated $[Pt(Pr'_3)_2]$ species likely via the precoordination[4] of $R_2P(S)H$ through either the sulfur or the phosphorus atom. The resulting $[PtH(PR'_3)_2\{P(S)R_2\}]$ intermediates exist as low temperatures in solution as a mixture of the trans (**1a**) and cis (**1b**) isomers in the case of $PR'_3 = PMePh_2$ and $R_2P(S)^- = Ph_2P(S)^-$. **1b** probably arises from a trans → cis rearrangement. Examination of the NMR data for **1a** and **1b** indicates that the trans influence of the ligands follows the order H > $P(S)Ph_2$ > $PMePh_2$. In light of this sequence the driving force for the trans → cis rearrangement may stem from bringing the ligands of the highest trans influence into mutual cis positions.

Increasing temperature leads to fast dissociation (on the NMR time scale) of the Pt–$PMePh_2$ bond in both **1a** and **1b**. It is obvious from the NMR spectra that for **1b** the dissociation of the $PMePh_2$ ligand trans to the hydride occurs as expected from its high trans influence. This dissociation process generates either a transient tricoordinated 14-electron species or a tetracoordinated 16-electron species as a result of the η^2 mode of bonding of the Ph_2PS^- ligand. The final products of the $[Pt(PR'_3)_4]/R_2P(S)H$ reactions, the bis(thiophosphinito)-bridged diplatinum(I) complexes, are slowly generated by H_2 evolution above −10 °C by reductive dimerization either from the 14- or 16-electron species or via an intermediate diplatinum(II) complex.

These results support an oxidative-addition step for both processes given by eq 1 and 2 through the common $[PtH(PR'_3)_2\{P(E)R_2\}]$ intermediate. The different final products of the reactions appear to arise from subsequent steps that are goverened by the tendency of the ligand either to form the hydrogen-bridged $(Ph_2PO\cdots H\cdots OPPh_2)^-$ species (E = O) or to function as a bridging group $(\mu\text{-}EPR_2)^-$ (E = S, Se).

The mechanism of the trans → cis rearrangement reaction and the H_2-release step deserve further study. Kinetic measurements will be undertaken to explore these steps.

---

(19) Zschunke, A.; Meyer, H.; Heidlas, I.; Messbauer, B.; Walther, B.; Schadler, H.-D.; Thomas, B. *Z. Anorg. Allg. Chem.* **1983**, *504*, 117.

In the course of the $[Pt(P\text{-}t\text{-}Bu_3)_2]/Ph_2(S)H$ reaction, the trans → cis rearrangement $[PtH(P\text{-}t\text{-}Bu_3)_2\{P(S)Ph_2\}]$ appears unlikely for steric reasons. **2** should be generated from the trans intermediate or its dissociation product $[PtH(P\text{-}t\text{-}Bu_3)(SPPh_2]$. The stability of **2** against H_2 release may be interconnected with the hindered trans → cis rearrangement or the boat conformation of **2**.

Registry No. **1a**, 96617-58-2; **1b**, 96648-01-0; **2**, 96633-12-4; Pt-$(PMePh_2)_4$, 27121-53-5; $Pt(P\text{-}t\text{-}Bu_3)_4$, 96617-59-3.

Supplementary Material Available: A packing diagram and full listings of interatomic distances and angles, anisotropic thermal parameters, hydrogen atom positional parameters, least-squares planes, and observed and calculated structure amplitudes (18 pages). Ordering information is given on any current masthead page.

Contribution from the Department of Chemistry,
Wayne State University, Detroit, Michigan 48202

Reactions of Coordinated β-Polyketonate Ligands. 2. Ligand Oxidation and Benzilic Acid Type Rearrangement in the Nickel(II) Complex of 2,2-Dimethyl-3,5,7-octanetrione. Molecular Structure of the Binuclear Nickel(II) Complex of the Resultant 2-*tert*-Butyl-2-hydroxy-3,5-dioxohexanoic Acid

R. L. LINTVEDT,* G. RANGER, and C. CECCARELLI

Received June 21, 1984

The trinuclear Ni(II) complex of 2,2-dimethyl-3,5,7-octanetrione, H_3PAA, was prepared and characterized as $Ni_3(PAA)_2(OH)_2(CH_3OH)_4$. Crystallization of this product from pyridine in air results in ligand oxidation and migration of the *tert*-butyl group from the 3- to the 4-carbon in a benzilic acid type rearrangement. The binuclear Ni(II) complex recovered contains the new ligand 2-*tert*-butyl-2-hydroxy-3,5-dioxohexanoate (2−), $t\text{-}BHMA^{2-}$, with a molecular formula $Ni_2(t\text{-}BHMA)_2(py)_4$. The blue crystals obtained are suitable for single-crystal X-ray studies. They contain, in addition to two Ni(II) ions, two *t*-BHMA dianions, four coordinated pyridine molecules, one pyridine, and three waters of solvation. The crystal belongs to the triclinic space group P_I and has 2 asymmetric molecules per unit cell. The lattice constants are $a = 10.324$ (3) Å, $b = 15.646$ (3) Å, $c = 16.018$ (5) Å, $\alpha = 87.00$ (2)°, $\beta = 79.45$ (2)°, $\gamma = 75.86$ (2) Å, and $V = 2466$ (1) Å^3. The structure was refined by least-squares analysis to a discrepancy factor of $R = 0.062$ for 2927 independent diffractometer data. The coordination sphere of each Ni(II) consists of two cis pyridine nitrogens, two enolate oxygens from the β-diketonate moiety of one $t\text{-}BHMA^{2-}$, and one carboxylate and a hydroxy oxygen from the second $t\text{-}BHMA^{2-}$, forming a five-membered chelate ring. The two nickel atoms are about 5.5 Å apart. A proposed mechanism for the ligand reaction is presented that depends upon initial oxidation at the 4-carbon to yield an σ-diketone as a precursor to the *tert*-butyl rearrangement. No ligand reaction is observed when the initial trinuclear complex is crystallized from pyridine in an inert atmosphere.

Introduction

The β-polyketones are a versatile class of ligands that constitute an homologous series capable of forming an homologous series of transition-metal complexes. The series members 1,3,5-triketones and above afford the opportunity to systematically assess the consequences of having two or more metal ions in close proximity on the chemical and physical properties of these molecular complexes. One of our fundamental interests in this class of compounds is to investigate the chemical significance of placing two or more metal ions in juxtapositions that allow for reasonably strong electronic/magnetic interactions. In this regard, one of the first general class of reactions to consider is the reaction of the ligand itself. Such reactions are interesting of themselves, but they are also important if the complexes are to be useful as potential reagents and/or catalysts, since the reactivity of the ligands may present competing reactions and destruction of the reagent or catalyst. Understanding ligand reactivity is important in the design of molecules for specific reactive purposes so that synthetic strategies may be planned to either block it or enhance it.

The oxidation of coordinated β-polyketonates has not been discussed in any detail. Complexes of the simplest and most familar homologues, the 1,3-diketones, do not appear to be particularly susceptible to ligand oxidation, since solutions of complexes with metal ions in normal oxidation states are routinely handled in air without difficulty. Since oxidation at the 2-carbon of 1,3-diketonates would result in decomposition of the chelate, such reactions would be obvious if they were important. Oxidation of the 1- or 3-carbons to carboxylates in the 1,3-diketonates does not appear to be of significance either. Incorporation of the 1,3-diketone into a macrocyclic ligand by condensation with a tetraamine and subsequent complexation with Co(II) yield a molecular ion in which the 2-carbon is readily oxidized to a carbonyl.[1-3] The oxidized species are isolated intact. Decomposition that would normally take place once the diketonate is oxidized is prevented by the macrocyclic nature of the complex. We have observed a similar type of oxidation at the 4-carbon of bis(1,7-diphenyl-1,3,5,7-heptanetetraonato)dicobalt(II) upon crystallization from 10% pyridine–90% benzene in air. The Co(II) ions are bound in the 1,3- and 5,7-positions, leaving the central position (3,5) empty. Oxidation of the 4-carbon to a carbonyl does not destroy the dianionic character of the ligand and, therefore, the complex. The structure of the oxidized molecule has been reported.[4] This study and the one reported herein are, to our knowledge, the only reports of oxidations of coordinated ligands involving higher homologues of β-polyketones. In both cases the reactions are sensitive to the number and kind of metal ions present.

Experimental Section

Synthesis of Bis(2,2-dimethyl-3,5,7-octanetrionato)dihydroxotetrakis(methanol)trinickel(II), $Ni_3(PAA)_2(OH)_2(CH_3OH)_4$. A solution containing 1.00 g (5.4×10^{-3} *m*) of 2,2-dimethyl-3,5,7-octanetrione, H_2PAA, and 1.07 g (1.46 mL) of $(C_2H_5)_3N$ in 50 mL of MeOH was heated to reflux. A solution of 1.62 g (6.51×10^{-3} *m*) of $Ni(H_3C_2O_2)_2(H_2O)_2$ in

---

(1) Weiss, M. D.; Goedken, V. L. *J. Am. Chem. Soc.* **1976**, *98*, 1976.
(2) Durham, B.; Anderson, T. J.; Switzer, J. A.; Endicott, J. F.; Glick, M. D. *Inorg. Chem.* **1977**, *16*, 271.
(3) Switzer, J. A.; Endicott, J. F. *J. Am. Chem. Soc.* **1980**, *102*, 80.
(4) Lintvedt, R. L.; Ranger, G.; Ceccarelli, C. *Inorg. Chem.* **1985**, *24*, 456.
(5) The abbreviation is based upon a trivial nomenclature commonly used for β-polyketones in which the compounds are treated as derivatives of simple ketones. In this case, $t\text{-}BHMA^{2-}$ stands for *tert*-butylhydroxymalonylacetonato.
(6) Cromer, D. T.; Waber, J. T. "International Tables for X-ray Crystallography"; Ibers, J. A., Hamilton, W. C., Eds.; Kynoch Press: Birmingham, England, 1974; Vol. IV, pp 71–147.
(7) Reference 6, pp 148–51.
(8) Steward, R. F.; Davidson, E. K.; Simpson, E. T. *J. Chem. Phys.* **1965**, *42*, 3175.

0020-1669/85/1324-2359$01.50/0